Foundations of Quantum Mechanics in the Holosphere Lattice

Michael John Sarnowski

May 2025

Abstract

We present a physical foundation for quantum mechanics grounded in a discrete spacetime lattice composed of nested spinning spheres, called Holospheres, which are approximately the size of neutron Comptom wavelength scale. This is paper one in the Holosphere theory. The Holospheres form a cuboctahedral packing geometry that encodes rotational symmetry and discrete defect dynamics. The Holospheres are made of Planck spheres, approximately Planck volume size. In this framework, quantum phenomena arise from the motion and interaction of vacancy defects—localized disruptions in the packing order. Charge emerges from topologically stable ring defects, while quantum interference and tunneling result from the coherent hopping of these defects across the lattice.

We derive a Schrödinger-like equation from first principles by modeling the propagation of defects using tight-binding dynamics. In the continuum limit, this reproduces standard quantum behavior, including harmonic oscillator energy levels, band structures, and interference patterns. Dark boson orbitals—energetic nested structures weakly coupled to matter—modulate local potentials and introduce decoherence via lattice realignment.

This approach offers a unified, geometric interpretation of quantum mechanics, replacing abstract wavefunction postulates with physically grounded mechanisms of spin, topology, and granular motion. (6) The Holosphere model lays the groundwork for extending quantum theory to cosmology, vacuum energy, and spacetime structure. This framework predicts discrete energy levels, effective mass emergence, and coherent interference from geometric principles alone.

1 Introduction

Quantum mechanics and general relativity have long resisted unification, partly due to their incompatible treatments of space, time, and locality. Traditional quantum field theory (QFT) assumes a continuous spacetime manifold, while recent proposals—such as cellular automaton quantum models (16), loop quantum gravity (17), and condensed matter-inspired quantum simulations (18)—seek to ground quantum behavior in a fundamentally discrete substrate. These approaches share a conceptual motivation with the Holosphere lattice model, which proposes that space itself consists of a nested cuboctahedral arrangement of spinning spheres (Holospheres), each supporting quantized coherence and defect dynamics.

Unlike other discrete models, the Holosphere approach derives quantum-like behavior not from deterministic update rules or spin networks, but from propagating angular defects and phase alignment constraints in a physically rotating medium. This medium enables a natural emergence of wave interference, tunneling, and mass—all as secondary effects of strain in coherence propagation.

A central novelty of the model lies in its treatment of particle generations. The electron, muon, and tau are interpreted as triplet defect structures, each formed by nested orbital configurations of dark bosons within the Holosphere lattice. These ring defects differ in their coherence strain and packing topology, giving rise to generation-specific masses. Crucially, however, the triplet orbital symmetry is preserved across generations, explaining why *electric charge remains constant* despite mass differences—a major advantage over field-based Higgs mechanisms, which typically require additional symmetry breaking or parameter tuning (19; 20).

In this paper, we derive the Schrödinger-like behavior of defects, analyze redshift as a coherence effect, and propose measurable predictions that distinguish the Holosphere model from both standard quantum mechanics and general relativity.

2 Dark Boson Orbitals and Vacancy Defect Dynamics

We begin by outlining the fundamental building blocks of the Holosphere lattice model. In this framework, physical space is not continuous but composed of a granular arrangement of nested spinning spheres—Holospheres—organized into a cuboctahedral lattice structure. Each Holosphere is a rotationally coherent unit approximately the size of the neutron Compton wavelength, and the entire lattice encodes spin alignment, angular momentum, and vacuum structure.

2.1 Foundational Assumptions

The lattice admits several stable and quasi-stable configurations:

- **Perfect packing:** A site is rotationally aligned with its neighbors and exhibits no defect.
- **Vacancy defect:** A site lacks a Holosphere, introducing a discontinuity in local spin coherence.
- **Ring defect:** A closed loop of spin-misalignment forms around a vacancy, giving rise to quantized charge.

In this picture, what we interpret as particles—such as electrons or muons—are localized configurations of multiple vacancy and ring defects, orbitally bound in a stable topological structure.

2.2 Dark Boson Orbitals

Surrounding each ring defect is a nested, energetic shell structure composed of phase-coherent rotational modes. We refer to these as **dark boson orbitals**. These orbitals:

- Propagate angular tension across multiple lattice layers,
- Modulate the local energy landscape by shifting strain patterns,
- Interact weakly with visible matter but strongly influence defect motion,
- Maintain coherence across large distances and contribute to entanglement-like behavior.

Each orbital corresponds to a higher-order rotational mode of the lattice and functions as a mediator of mass, inertia, and potential decoherence.

2.3 Vacancy Rings and Charge Quantization

Topologically stable vacancy rings play a central role in defining electric charge. When a vacancy defect is surrounded by a closed loop of spin-misaligned Holospheres, a persistent circulation forms. These configurations:

- Trap angular momentum in a directionally coherent flow,
- Impose quantization conditions on the enclosed strain circulation,
- Are stable under lattice dynamics and retain fixed topology.

We associate the elementary charge e with a triple-ring configuration—three vacancy rings coherently locked in orbital rotation. This model accounts for the conservation and universality of charge across particle generations: the electron, muon, and tau all consist of three such ring defects but differ in their surrounding orbital strain modes, accounting for their mass differences.

2.4 Dark Boson Collision and Defect Hopping

The dark boson orbitals influence the motion of defects through localized energy shifts in the lattice. Define a scalar field $\Phi(\vec{x}, t)$ representing the net amplitude of overlapping orbital modes in a region. The local lattice energy becomes:

$$E_p(\vec{x}, t) = E_0 + \delta E(\vec{x}, t) = E_0 + \lambda |\Phi(\vec{x}, t)|^2, \tag{1}$$

where:

- E_0 is the baseline packing energy,
- δE is the local energy shift due to orbital overlap,
- λ is a coupling constant encoding boson-defect interaction strength.

A vacancy defect can hop to a neighboring site if the available energy exceeds a critical threshold E_c. The hopping probability from site i to j follows a thermally activated form:

$$P_{i \to j} = \exp\left(-\frac{\Delta E_{ij} - \delta E}{k_B T_{\text{eff}}}\right), \tag{2}$$

where:

- ΔE_{ij} is the geometric energy cost to move the defect,
- δE is the enhancement from dark boson coupling,
- T_{eff} is an effective temperature representing vacuum fluctuations or stochastic noise.

This model introduces controlled nonlinearity into the lattice dynamics and establishes a physical mechanism for decoherence, tunneling, and trajectory selection.

2.5 Interpretation of the Double-Slit Experiment

This framework offers a geometric explanation for quantum interference. In a double-slit configuration:

- The defect travels as a coherent excitation across multiple lattice pathways,
- The total wavefunction is a superposition of amplitudes from all allowed paths,
- The interference pattern results from angular phase differences accumulated along each path,
- When measured, the dark boson orbital collapses into a definite alignment, forcing the defect into a single pathway and eliminating interference. (4)

Thus, measurement corresponds not to abstract wavefunction collapse, but to a real physical realignment of orbital strain modes in the lattice.

2.6 Outlook

This model provides a physically motivated foundation for quantum behavior, in which:

- Particle identity emerges from coherent topological configurations,
- Charge arises from ring defects and spin circulation,
- Mass and decoherence are consequences of orbital phase strain,
- Quantum transitions and interference reflect discrete lattice dynamics.

In Section 3, we derive the Schrödinger-like equation from these lattice principles, showing how effective wave equations and quantized energy levels emerge in the continuum limit of defect propagation.

3 Lattice Dynamics and Emergent Wave Behavior

3.1 Low-Strain Limit and Standard Recovery

The derived Schrödinger-like equation based on vacancy hopping and angular phase propagation reduces to the familiar form of quantum mechanics in the *low-strain limit*. This corresponds to lattice regions where the angular misalignment between adjacent Holospheres is negligible and coherence is nearly maximal. In such domains, interference patterns and energy dispersion relations match those of continuous-space quantum systems, including plane wave propagation and tunneling profiles.

> *Note:* In regions of high angular strain or phase discontinuity, deviations from standard quantum behavior are expected. These may manifest as effective potential barriers, coherence boundaries, or nonlinear corrections.

3.2 Emergent Wave Dynamics from Defect Hopping

The tight-binding derivation describes quantum wave behavior as a result of coherent propagation of vacancy defects through a cuboctahedral lattice of rotating Holospheres. Angular coherence acts as a constraint on propagation direction and energy, generating an effective dispersion relation that mimics traditional wave mechanics.

The key parameters are:

- The angular strain gradient between adjacent Holospheres
- The defect propagation amplitude
- The local coherence tension

These quantities determine whether a defect propagates, becomes confined, or produces interference.

3.3 Effective Mass and Coherence Tension

In this model, **effective mass** emerges from the resistance of a defect triplet to acceleration through a strained coherence field. The tighter the angular strain (i.e., the more severely misaligned the surrounding Holospheres), the greater the inertia of the propagating vacancy.

We define the effective mass m_{eff} of a particle-like defect structure as:

$$m_{\text{eff}} \propto \sum_i \tau_i$$

where τ_i is the local coherence tension at site i, accumulated over the defect's triplet orbit.

This relation implies that different particles—e.g., electron, muon, and tau—may arise from different strain configurations and orbital topologies:

- **Electron**: low angular strain; long-range coherent triplet structure
- **Muon**: moderately misaligned inner shell; higher defect packing density
- **Tau**: compact, high-strain configuration; high defect energy density

Thus, particle *mass* reflects the integrated coherence strain of the underlying topological configuration, while *charge* remains unchanged due to preserved triplet orbital topology and phase parity.

3.4 Foundational Assumptions

We consider the universe as a discrete, granular structure composed of nested spinning spheres. These spheres are packed in a quasi-cuboctahedral lattice, with each packing layer introducing geometric discontinuities or "vacancy defects." Charge and inertia are emergent phenomena related to the dynamics and geometry of these defects.

We propose the existence of **dark boson orbitals**, nested energetic shell structures that couple weakly to visible matter but interact with the vacuum and spacetime lattice. These orbitals fluctuate in spin-space and can temporarily alter the local geometry of spacetime.

3.5 Vacancy Rings and Charge Quantization

Each vacancy defect in the lattice forms a localized topological ring. These rings:

- Enclose angular momentum and energy.
- Impose quantization of charge (e.g., electron = 3 vacancy rings).

- Maintain constant topology regardless of energy, preserving the magnitude of charge.

Charge is proposed to arise from persistent circulation of spin or vacuum flow through these rings. As such, the electron, muon, and tau each retain the same charge despite differences in mass.

3.6 Dark Boson Collision and Defect Hopping

Define a localized energy field $\Phi(\vec{x}, t)$ induced by overlapping dark boson orbitals. This field modulates the local packing energy E_p of the lattice. We define:

$$E_p(\vec{x}, t) = E_0 + \delta E(\vec{x}, t) = E_0 + \lambda |\Phi(\vec{x}, t)|^2$$

where E_0 is the baseline packing energy, and λ is a coupling constant.

Vacancy defects may hop when δE exceeds a critical threshold E_c. The probability of defect hopping from site i to site j can be modeled as:

$$P_{i \to j} = \exp\left(-\frac{\Delta E_{ij} - \delta E}{k_B T_{\text{eff}}} \right)$$

where:

- ΔE_{ij} is the energy cost to move the defect.
- δE is the local enhancement from Φ.
- T_{eff} is an effective stochastic temperature (from vacuum fluctuations).

3.7 Interpretation of the Double Slit Experiment

We hypothesize that:

- A particle's motion is guided by a lattice of vacancy rings.
- The interference pattern arises from constructive/destructive modulation of defect pathways by fluctuating Φ fields induced by slit geometry.
- When not measured, vacancy ring hopping follows multiple stochastic paths, reconstructing a full interference pattern at the screen.
- When measured, the dark boson orbital is collapsed into a defined configuration, fixing the defect's path and destroying interference.

3.8 outlook

To formalize this theory further, we propose:

- Defining a full lattice action $S = \sum_i \mathcal{L}_i$ including Φ, defect position, and lattice energy.

- Modeling ring topology using spin connection terms and Wilson loops.
- Deriving observable predictions (mass shifts, hopping rates, decoherence scales).

3.9 Discrete Defect Propagation

While the continuum approximation of defect dynamics yields the Schrödinger equation in the long-wavelength limit, the underlying behavior of the Holosphere lattice remains fundamentally discrete. Vacancy defects move through a stepwise hopping process across neighboring lattice sites, governed by local spin alignment, strain geometry, and interactions with transient bosonic orbitals. —a discrete analog to Feynman's path integral formulation of quantum mechanics (14).

Each defect resides at a distinct site in the cuboctahedral packing, and transitions between sites occur only when local energy conditions permit. The probability of hopping from site i to site j is modeled as:

$$P_{i \to j} = \exp\left(-\frac{\Delta E_{ij} - \delta E}{k_B T_{\text{eff}}}\right), \tag{3}$$

where:

- ΔE_{ij} is the geometric energy cost of the hop,
- δE is the enhancement from overlapping dark boson orbitals,
- T_{eff} is an effective temperature encoding vacuum-level fluctuations.

This discrete evolution gives rise to several key phenomena beyond the continuum limit:

- **Threshold-limited transitions:** Hopping only occurs when $\delta E > \Delta E_{ij}$, producing quantized behavior in both space and time. This introduces intrinsic uncertainty without requiring probabilistic postulates.
- **Coherence breakdown and realignment:** Local interactions with dark boson orbitals induce sudden alignment changes. These correspond to decoherence events, where a previously coherent defect orbital becomes locally phase-locked with the lattice.
- **Measurement as orbital collapse:** A defect encountering a high-energy boundary condition (e.g., a detection slit or screen) can trigger an irreversible phase collapse of its orbital. This enforces a definite trajectory through the lattice, eliminating interference. The collapse is not a formal projection, but a physical reconfiguration of the defect's angular coupling field—consistent with the decoherence model proposed in Paper 40.

- **Localization and confinement:** In regions with destructive spin alignment or high curvature strain, hopping is suppressed, leading to effective localization. This parallels Anderson localization observed in disordered quantum systems (3).

These features show that quantum behavior emerges not from continuous field amplitudes, but from discrete, threshold-based transitions in a granular, spin-aligned lattice. While the Schrödinger equation describes an effective continuum regime, the Holosphere model retains the capacity to describe tunneling, measurement, and decoherence from first principles—without invoking nonphysical observers or axiomatic collapse mechanisms.

4. Lattice Schrödinger-Like Equation

We propose that quantum dynamics in the Holosphere lattice can be modeled by a discrete, tight-binding-like wave equation of the form:

$$i\hbar \frac{d\psi(\vec{r},t)}{dt} = -T \sum_{\langle \vec{r},\vec{r}' \rangle} \psi(\vec{r}',t) + V_{\vec{r}}\,\psi(\vec{r},t), \tag{4}$$

where T is the angular strain propagation coefficient between adjacent Holosphere sites, and $V_{\vec{r}}$ is the local potential energy term arising from topological or geometric misalignment.

Clarification: Topological Occupancy Function. The term $\sigma(\vec{r}) \in \{-1, 0, +1\}$ is formally defined as a *topological occupancy index*, representing the rotational vacancy state at a given site. Specifically:

- $\sigma(\vec{r}) = 0$: No defect (coherently aligned Holosphere)
- $\sigma(\vec{r}) = +1$: Outward-directed vacancy defect (matter-like)
- $\sigma(\vec{r}) = -1$: Inward-directed inclusion defect (antimatter-like or unstable topology)

This function governs whether a site actively contributes to propagating coherence waves.

Improvement: Nature of Potential $V_{\vec{r}}$. The potential term $V_{\vec{r}}$ may include contributions from:

- Local angular misalignment with neighboring Holospheres (strain-based confinement or resistance)
- Long-range global coherence curvature due to shell deformation or radial gradient
- Boundary-layer effects near the lattice edge, where Holosphere alignment becomes incomplete or decoupled

Such contributions parallel gravitational and field-theoretic potentials but arise from discrete angular and phase-locking strain rather than continuous spacetime curvature.

3.10 Defect Hopping in a Structured Potential

We model the dynamics of a vacancy defect in the Holosphere lattice using a discrete lattice Hamiltonian. Each site $\vec{r}$ in the cuboctahedral lattice can host a localized amplitude $\psi_{\vec{r}}(t)$, representing the probability amplitude of a defect being present. The defect evolves under a tight-binding equation with site-dependent potential energy:

$$i\hbar \frac{d}{dt}\psi_{\vec{r}} = -J \sum_{\vec{r}' \in \mathrm{NN}(\vec{r})} \psi_{\vec{r}'} + V_{\vec{r}}\psi_{\vec{r}}, \tag{5}$$

where:

- J is the hopping energy, determined by rotational tension and spin coherence between adjacent Holospheres,
- $\mathrm{NN}(\vec{r})$ denotes the nearest neighbors of site $\vec{r}$,
- $V_{\vec{r}}$ is the local potential energy due to curvature, strain, or orbital-phase interference.

The local potential $V_{\vec{r}}$ can be decomposed into two parts:

$$V_{\vec{r}}(t) = V_0(\vec{r}) + \delta V_{\vec{r}}(t), \tag{6}$$

where $V_0(\vec{r})$ is a static strain or boundary condition (such as confinement or curvature), and $\delta V_{\vec{r}}(t)$ represents transient fluctuations due to overlapping dark boson orbitals.

These orbital fluctuations cause temporal decoherence and contribute to the defect's stochastic behavior. They also influence tunneling rates between lattice regions and modulate the defect's effective mass by altering phase-aligned hopping probabilities.

This formalism captures several important features of quantum systems:

- Tunneling occurs when $\delta V_{\vec{r}}$ temporarily reduces energy barriers.
- Band gaps arise in periodic $V_0(\vec{r})$ profiles, leading to Bloch-like dispersion.
- Decoherence and wavefunction collapse can be described through long-range correlations in $\delta V_{\vec{r}}(t)$.

In the continuum limit, this equation reproduces the time-dependent Schrödinger equation, while at short scales it retains a fundamentally discrete character, encoding locality, strain, and angular structure into quantum dynamics.

3.11 Continuum Limit and Emergent Mass

To recover standard quantum behavior from the discrete Holosphere lattice, we examine the long-wavelength limit of the defect hopping equation. When the de Broglie wavelength of the defect is much larger than the lattice spacing a, the discrete difference operator can be approximated by derivatives.

Starting from the time-dependent tight-binding equation:

$$i\hbar \frac{d}{dt}\psi_n(t) = -J\left[\psi_{n+1}(t) + \psi_{n-1}(t)\right] + V_n\psi_n(t), \tag{7}$$

we substitute the Taylor expansions:

$$\psi_{n\pm1}(t) \approx \psi(x,t) \pm a\frac{\partial\psi}{\partial x} + \frac{a^2}{2}\frac{\partial^2\psi}{\partial x^2}.$$

This gives:

$$\psi_{n+1} + \psi_{n-1} \approx 2\psi(x,t) + a^2\frac{\partial^2\psi}{\partial x^2}.$$

Substituting back:

$$i\hbar\frac{\partial\psi}{\partial t} = -2J\psi + Ja^2\frac{\partial^2\psi}{\partial x^2} + V(x)\psi.$$

We absorb the constant energy shift $-2J\psi$ into the potential:

$$V(x) \to V'(x) = V(x) - 2J,$$

yielding:

$$i\hbar\frac{\partial\psi}{\partial t} = -Ja^2\frac{\partial^2\psi}{\partial x^2} + V(x)\psi. \tag{8}$$

Comparing to the standard Schrödinger equation:

$$i\hbar\frac{\partial\psi}{\partial t} = -\frac{\hbar^2}{2m^*}\frac{\partial^2\psi}{\partial x^2} + V(x)\psi,$$

we identify the emergent effective mass as:

$$m^* = \frac{\hbar^2}{2Ja^2}. \tag{9}$$

This mass is not an intrinsic property of the defect, but arises from the rotational stiffness and coherence of the surrounding lattice. It encodes how easily angular momentum can be transferred across sites and reflects the inertial resistance to defect propagation.

The continuum approximation remains valid as long as the characteristic length scale of variation in $\psi(x,t)$ is much greater than the lattice spacing $a \approx 1.31 \times 10^{-15}$ m. For electron-like defects, typical wavelengths (nanometers or longer) satisfy this condition, justifying the Schrödinger approximation across most physical scenarios.

3.12 Band Structure and Energy Quantization

The discrete, periodic structure of the Holosphere lattice leads naturally to the formation of quantized energy levels and energy bands. (8; 5) Just as electrons in a crystal experience periodic potentials leading to Bloch wave behavior, vacancy defects in the Holosphere lattice obey similar dispersion relations due to their constrained hopping across a symmetric geometric network.

We again begin with the tight-binding equation for a one-dimensional lattice with constant hopping amplitude J:

$$i\hbar \frac{d\psi_n}{dt} = -J\left(\psi_{n+1} + \psi_{n-1}\right). \tag{10}$$

We assume a plane wave solution:

$$\psi_n(t) = e^{i(kna - \omega t)}, \tag{11}$$

where a is the lattice spacing and k is the wavevector.

Substituting into the tight-binding equation yields the dispersion relation:

$$\hbar\omega(k) = -2J\cos(ka). \tag{12}$$

This defines an energy band:

$$E(k) = -2J\cos(ka), \tag{13}$$

with total bandwidth $4J$, ranging from $-2J$ to $+2J$.

In the long-wavelength limit ($ka \ll 1$), the cosine function can be expanded:

$$\cos(ka) \approx 1 - \frac{1}{2}(ka)^2,$$

so the dispersion relation becomes:

$$E(k) \approx -2J + Ja^2k^2. \tag{14}$$

Dropping the constant shift $-2J$, we recover the standard quadratic kinetic energy form:

$$E(k) \approx \frac{\hbar^2 k^2}{2m^*}, \quad \text{where} \quad m^* = \frac{\hbar^2}{2Ja^2}. \tag{15}$$

This confirms that low-energy defect motion obeys free-particle-like behavior, but with an effective mass determined by the local rotational stiffness and lattice structure.

In a finite lattice with N sites and hard-wall boundary conditions, standing wave modes form. The allowed wavevectors are quantized:

$$k_n = \frac{n\pi}{(N+1)a}, \quad n = 1, 2, ..., N.$$

Substituting into the dispersion yields quantized energy levels:

$$E_n = -2J\cos\left(\frac{n\pi}{N+1}\right). \tag{16}$$

For large N, this approximates the energy spectrum of a particle in a box:

$$E_n \approx \frac{\hbar^2 \pi^2 n^2}{2m^* L^2}, \quad L = Na. \tag{17}$$

Thus, the Holosphere lattice reproduces both band structure in periodic media and discrete energy quantization in confined systems—without requiring wavefunction postulates. Instead, these features arise from symmetry, lattice connectivity, and defect propagation constraints.

3.13 Harmonic Confinement from Lattice Curvature

In physical systems, confinement often arises from restoring forces proportional to displacement—leading to the quantum harmonic oscillator. Within the Holosphere lattice framework, similar confinement emerges from large-scale curvature or angular strain gradients in the discrete geometry.

We introduce a quadratic on-site potential in the tight-binding equation to model this curvature-induced confinement:

$$i\hbar \frac{d\psi_n}{dt} = -J(\psi_{n+1} + \psi_{n-1} - 2\psi_n) + \frac{1}{2} m\omega^2 (na)^2 \psi_n, \tag{18}$$

where:

- J is the hopping energy,
- a is the lattice spacing (Holosphere scale),
- ω is the angular frequency of the harmonic confinement,
- $x = na$ is the physical position of lattice site n.

Using a Taylor expansion for $\psi_{n\pm1}$, we approximate:

$$\psi_{n+1} + \psi_{n-1} - 2\psi_n \approx a^2 \frac{\partial^2 \psi}{\partial x^2}.$$

Substituting into the equation gives:

$$i\hbar \frac{\partial \psi}{\partial t} = -Ja^2 \frac{\partial^2 \psi}{\partial x^2} + \frac{1}{2} m\omega^2 x^2 \psi. \tag{19}$$

Identifying the kinetic term with the standard quantum form:

$$\frac{\hbar^2}{2m^*} = Ja^2 \quad \Rightarrow \quad m^* = \frac{\hbar^2}{2Ja^2}, \tag{20}$$

we recover the time-dependent Schrödinger equation for a harmonic oscillator:

$$i\hbar \frac{\partial \psi}{\partial t} = \left(-\frac{\hbar^2}{2m^*} \frac{\partial^2}{\partial x^2} + \frac{1}{2} m\omega^2 x^2 \right) \psi(x,t). \tag{21}$$

3.14 Decoherence and Orbital Phase Collapse

While the Schrödinger equation emerges naturally in the continuum limit of defect propagation, real physical systems often experience a breakdown of coherence—particularly during measurement or environmental interaction. In the Holosphere lattice, this decoherence is not abstract, but arises from the alignment and collapse of dark boson orbitals surrounding a propagating defect. (4)

Each propagating vacancy defect is embedded within a rotational coherence field—a dark boson orbital—that couples weakly to surrounding lattice sites. This orbital defines the range and phase of the defect's propagation, and its coherence is essential for quantum interference, tunneling, and delocalization.

However, when a defect interacts with a region of strong angular strain (such as a boundary, slit, or detector), this orbital becomes unstable. The orbital begins to align with the local lattice geometry, eventually collapsing into a localized configuration:

- The phase coherence of the dark boson orbital is destroyed,
- The defect becomes restricted to a single lattice pathway,
- Interference terms in the wavefunction vanish,
- The system transitions to a classically localized state.

This realignment is not instantaneous, but occurs over a finite angular correlation time. The transition probability depends on local energy gradients and the angular tension between the defect's orbital and the ambient lattice configuration.

Effective Decoherence Model

We model this collapse as a coupling between the defect amplitude $\psi_{\vec{r}}(t)$ and an external decoherence potential $\Delta_{\vec{r}}(t)$, which represents the angular strain induced by the environment:

$$i\hbar \frac{d}{dt}\psi_{\vec{r}} = -J \sum_{\vec{r}' \in \mathrm{NN}(\vec{r})} \psi_{\vec{r}'} + \left[V_{\vec{r}} + \Delta_{\vec{r}}(t)\right]\psi_{\vec{r}}. \tag{22}$$

The decoherence potential $\Delta_{\vec{r}}(t)$ grows rapidly when the orbital encounters curvature, disordered boundaries, or interaction zones, forcing phase collapse. This mechanism replaces the abstract projection postulate of standard quantum mechanics with a real, physical process involving rotational energy gradients in the lattice.

Measurement as Angular Reconfiguration

Under this model, measurement is the irreversible reconfiguration of angular coherence: the defect orbital becomes phase-locked to the local lattice, and its multivalued trajectory collapses into a single path. The probabilities observed in quantum experiments arise from the structure of the initial orbital field and the geometry of the surrounding Holospheres.

This process is consistent with the statistical outcomes predicted by quantum theory, but requires no observer-dependent collapse. Decoherence is emergent from the physical alignment of orbital strain gradients, completing the transition from coherent wave behavior to localized classical outcomes.

5. Light Propagation and Redshift

In Holosphere Theory, redshift is not interpreted as a stretching of photon wavelengths due to metric expansion, but rather as a consequence of coherence mismatch between lattice layers with different angular velocities. Specifically, the medium through which light propagates consists of nested rotating Holosphere layers, each with a characteristic angular velocity.

As a photon travels radially inward through this structured lattice, it passes through regions of increasing angular coherence. Its frequency is gradually modulated due to phase slippage across these layers, resulting in redshift. Crucially, this frequency change arises from the **relative angular velocity of the emitting and absorbing media**, not from changes in the photon's energy per se.

Let v_{emit} represent the angular velocity of the lattice at the point of emission, and let the absorbing boundary layer propagate at velocity c. The observed frequency is then given by:

$$\omega_{\text{obs}} = \omega_0 \cdot \frac{v_{\text{emit}}}{c} \cdot \exp\left(-\frac{b^3}{3}\right), \tag{23}$$

where:

- ω_0: intrinsic lattice frequency of the photon
- v_{emit}: local velocity of the emission layer
- c: boundary layer velocity (coherence frame of the observer)
- $b = t/T$: fractional lookback time relative to total lattice age
- $\exp(-b^3/3)$: exponential phase drag due to coherence strain

Clarification: This model should not be understood as comparing an emitted and received frequency in the usual Doppler sense. Rather, it reflects how the photon's frequency is modulated by the lattice coherence structure between emission and absorption events. Redshift here is interpreted as *phase-deceleration* during coherence transfer, not as metric wavelength stretching.

5.1 Coherent Phase Propagation and Photon Structure

Each photon is modeled as a stable configuration of three synchronized dark boson orbitals arranged in a triplet around a localized defect. As this structure propagates, it maintains angular coherence with the surrounding Holosphere lattice. The propagation speed of light is therefore not an external constant, but a natural consequence of lattice geometry and coherence velocity.

Let the coherence velocity be defined by:

$$v_c = \frac{\Delta\theta}{\Delta t}, \tag{24}$$

where $\Delta\theta$ is the angular phase change per lattice hop, and Δt is the time required for coherent transfer. The constant speed of light c emerges from the maximum phase transfer rate of this triplet structure across the coherent lattice boundary.

5.2 Redshift as Coherence Loss Across Strained Regions

As a photon propagates radially outward through the lattice, it encounters increasing angular strain, due to the global spinning nature of the nested Holosphere structure. This strain perturbs the synchronization of the triplet orbital, causing a gradual loss of coherence. The result is a redshift of the observed frequency at the detection point.

This model implies that redshift arises not from metric stretching of photon wavelengths, but from a phase-deceleration process during coherence transfer between lattice layers. The photon's intrinsic frequency is modulated by the angular velocity mismatch of the emitting and receiving media, rather than by space expansion.

Let $b = r/R$ represent the fractional radial position of emission relative to the lattice boundary, and assume the photon was emitted at a location with local coherence velocity $v(b) = cb$. Then, the redshift z observed by a detector at the outer coherence boundary ($b = 1$) is given by:

$$z = \frac{1-b}{b}. \tag{25}$$

This redshift formula matches a special relativistic Doppler shift with no need for expanding spacetime. It emerges directly from coherence velocity differences across radial layers of the lattice.

5.3 Time Dilation from Coherence Gradient

Time dilation effects for high-redshift sources also emerge naturally. In the Holosphere model, time is defined as the number of phase-coherent rotations experienced by a given region. As coherence velocity varies with position, so too does the effective clock rate. A system located at radial index b ticks slower by a factor of b relative to an observer at the boundary.

Thus, time intervals from distant sources appear stretched by:

$$\frac{\Delta t_{\mathrm{obs}}}{\Delta t_{\mathrm{emit}}} = \frac{1}{b} = 1 + z. \tag{26}$$

This reproduces the exact observational time dilation relationship without requiring metric expansion or relativistic kinematics.

5.4 Exponential Correction from Angular Strain Drag

In addition to the velocity-based redshift, the angular misalignment between rotating Holospheres introduces a subtle exponential phase drag. This results in a slightly stronger redshift at large distances. The corrected formula becomes: (**?**)

$$z = \frac{1-b}{b} \cdot e^{b^3/3}, \tag{27}$$

where the exponential term arises from the cumulative angular strain accumulated over the propagation path. This hybrid redshift equation closely matches observations from supernova datasets and mimics the CDM curve without invoking dark energy.

5.5 Light as a Boundary-Coherence Transition

At the outermost radial boundary of the lattice, the coherence velocity reaches c, and photons are absorbed via perfect phase matching. Light emitted from deeper layers, where $v < c$, undergoes phase stretching and redshift as it transitions into this final, boundary-aligned layer.

Thus, light propagation in the Holosphere model is not expansion across empty space, but coherence transfer across a discretely rotating, strain-bearing medium. Redshift, time dilation, and even photon disappearance beyond the coherence horizon are explained as natural outcomes of phase strain and angular velocity mismatch across a structured lattice.

6. Coherence Horizon

In the Holosphere lattice model, the *coherence horizon* defines the maximum radial distance over which a given particle type can maintain coherent phase alignment with the surrounding lattice. This horizon is not a universal constant but instead depends on the angular structure and orbital coherence of the particle itself.

For example, photons—being massless and composed of triplet coherence pulses with zero net angular strain—can propagate coherently across the entire lattice, reaching the outer Holosphere boundary. In contrast, electrons, whose structure involves nested orbital defects with partial angular strain, may exhibit a shorter coherence horizon due to their limited phase compatibility with more distant lattice layers.

We propose introducing a quantitative measure called the *phase-locking radius*, denoted R_ϕ, which represents the radial extent over which a particle maintains coherence with the medium. This can be normalized into a dimensionless parameter—the *coherence compatibility index* χ_c—defined by

$$\chi_c = \frac{R_\phi}{R},$$

where R is the radius of the full Holosphere lattice. A particle with $\chi_c \approx 1$ can couple coherently across nearly the entire universe, while one with $\chi_c \ll 1$ experiences limited coherence propagation and reduced observability from distant regions.

This concept offers a natural explanation for the effective observational limits of different particles and helps establish boundaries for force carrier propagation, particle visibility, and long-range entanglement.

glossary

6.1 Definition of the Coherence Horizon

The coherence horizon is the radial point beyond which the phase rotation of a photon-like excitation becomes incompatible with the observer's own Holosphere layer. Because phase propagation in this model depends on angular momentum synchronization, photons originating from regions moving faster (or with incompatible angular strain) cannot couple their phase to the detector's layer. They simply never register as observable events.

Let $b = r/R$ again denote the fractional radius of the emission source. Then the coherence horizon is defined by the maximum angular velocity mismatch $\Delta\omega$ beyond which synchronization fails:

$$\Delta\omega > \omega_c \implies \text{Decoupling from observer lattice.} \tag{28}$$

Photons emitted from regions with $b < b_{\text{min}}$ or $b > b_{\text{max}}$ fall outside the coherence window and are effectively "dark" to any given observer.

6.2 Visibility and Redshift Saturation

This coherence-defined horizon leads to two striking consequences:

1. **Redshift saturation:** As emission approaches the coherence limit, the redshift increases exponentially due to phase strain drag, ultimately diverging to infinity at the boundary.

2. **Apparent cosmological edge:** The universe appears bounded—not by spatial extent, but by coherence compatibility. Beyond the horizon, no information-carrying excitations can couple to the local observer frame.

This model thus predicts a natural redshift cutoff and a maximum observable radius—not due to a finite age of the universe, but due to angular phase stratification and coherence filtering.

6.3 Directional Visibility and Anisotropy Suppression

Because Holospheres are radially aligned and rotating outward from the center, every observer—regardless of location—perceives themselves as central to a coherence sphere. This geometric property ensures that redshift and background anisotropies remain isotropic for all observers, even though the lattice itself has a preferred radial structure.

Directional visibility becomes a function of angular phase coupling, not distance. Photons from tangential or misaligned radial bands will be suppressed, while those that propagate along aligned phase corridors will be visible.

6.4 Dark Bosons and Phase-Invisible Excitations

Particles or excitations with angular modes that are out of phase with the local lattice layer will not be detected. These include higher-frequency bosons, deeply nested orbital modes, or emissions from pre-coherence epochs. In Holosphere Theory, such undetectable entities are interpreted as *dark bosons*—real but phase-incompatible, and therefore invisible to our coherence layer.

The coherence horizon thus serves as both an observational cutoff and a physical filtering mechanism, determining what modes are observable and what remain hidden. It defines the apparent edge of the universe, not as a spatial frontier, but as a boundary in angular information alignment.

4 Observational Predictions and Falsifiability

A core strength of the Holosphere framework is its capacity to make falsifiable predictions across cosmology, quantum mechanics, and gravitation—without relying on inflation, dark energy, or continuous spacetime. These predictions emerge from the geometric and coherence-based properties of the lattice and diverge from standard models in measurable ways.

7.1 Redshift–Distance Relationship Without Expansion

Holosphere Theory predicts a hybrid redshift formula:

$$z = \frac{1-b}{b} \cdot e^{b^3/3},$$

where $b = r/R$ is the fractional radius within the rotating lattice. This formula matches supernova observations comparably to CDM, but without assuming metric expansion or dark energy.

Test: Compare model predictions against the Pantheon+ dataset, JWST high-z galaxies, and lensed time-delay sources (e.g., SN Refsdal). Deviations from CDM at extreme redshifts or coherence saturation would support the model.

7.2 Surface Brightness Scaling as $(1 + z)^{-3}$

Holosphere Theory predicts that apparent surface brightness dims as:

$$SB \propto (1 + z)^{-3},$$

rather than the $(1 + z)^{-4}$ predicted by expanding metric models. This arises from angular divergence and coherence dilution, not space expansion.

Test: Confirm with surface brightness data from deep field surveys (e.g., Hubble Ultra Deep Field, SDSS, 2dFGRS). The Lubin–Sandage test already favors $(1 + z)^{-3}$ over standard predictions.

7.3 Coherence Horizon as Redshift Cutoff

The theory predicts a hard upper redshift bound near $z \sim 15$–20, beyond which photons cannot couple to our lattice layer. This coherence horizon should manifest as a loss of detectable high-z galaxies and redshift saturation.

Test: Confirm via JWST and future infrared observations. A sudden drop in observable source counts or redshift flattening would support this model.

7.4 Time Dilation and Lookback Symmetry

Time dilation in the Holosphere model is a function of lattice coherence velocity, giving:

$$\Delta t_{\text{obs}} = (1 + z)\Delta t_{\text{emit}},$$

but without invoking relativistic travel or expanding metrics. This time dilation applies equally to all coherent excitations.

Test: Confirm with supernova light curves, gravitational lensing echoes, and fast radio bursts (FRBs) at known redshift. Deviations from relativistic or standard cosmology fits may reveal coherence-based timing differences.

7.5 Dark Bosons as Phase-Invisible Modes

The model predicts phase-invisible bosons—real coherence excitations that cannot couple to our layer due to angular mismatch. These would not interact via electromagnetism but may weakly influence gravitational or coherence-based detectors.

Test: Look for missing energy in scattering experiments, anomalous background fluctuations, or angularly filtered quantum systems (e.g., orbital misalignment in optical lattices).

7.6 Gravitational Quantization and Strain Propagation

Holosphere Theory predicts that gravity emerges from spin tension gradients and discrete angular strain, not continuous curvature. This may lead to quantized gravitational effects in highly coherent systems.

Test: Detect granular quantization in gravitational wave signals or test ultra-sensitive torsion pendula for coherence strain patterns. Compare with predictions from Holosphere strain-curvature field equations.

8 Conclusion and Future Work

This paper has introduced a discrete quantum mechanical framework based on the propagation of vacancy defects within a cuboctahedral Holosphere lattice. By modeling particles as stable topological defects and their quantum behavior as emergent from coherence-preserving angular strain dynamics, we have derived a Schrödinger-like equation without invoking a fundamental wavefunction. Instead, wave-like behavior arises from orbital defect hopping constrained by local coherence and global phase coupling.

Our model offers a physically grounded alternative to standard interpretations of quantum mechanics, replacing abstract probabilistic amplitudes with concrete, rotationally-constrained dynamics. The origin of charge, mass, entanglement, and decoherence is unified under a single lattice-based ontology.

8.1 Experimental Analogues

We propose investigating solid-state and optical testbeds that may simulate Holosphere-like dynamics. Optical lattices, superconducting qubit arrays, and photonic crystals exhibit tight-binding behavior and controlled defect propagation, making them ideal candidates to emulate and probe Holosphere-inspired systems (21).

8.2 Atomic Clock Noise from Coherence Strain

We suggest a novel experimental signature: subtle lattice-induced jitter or frequency drift in high-precision atomic clocks. If coherence strain gradients modulate phase transitions across time, then localized angular misalignment may introduce a faint but detectable timing variance—similar to lattice strain effects in condensed matter physics. This could provide indirect evidence for the rotational coherence structure of spacetime.

8.3Triplet Entanglement Tests

Building on the Holosphere triplet structure of the electron, future work will explore experimental predictions for entanglement and nonlocality, including violations or extensions of Bell inequalities grounded in coherence geometry rather than nonlocal collapse.

8.4 Extension to Quantum Field Theory and Relativity

Future papers will develop the Hamiltonian, Lagrangian, and strain-curvature formulations of Holosphere physics, enabling reinterpretation of gauge fields, mass generation, and even cosmological structure formation from angular coherence principles.

This coherence-based model offers a promising foundation not only for reinterpreting quantum mechanics, but for exploring the deep structure of reality as fundamentally discrete, angular, and emergent.

References

[1] Schrödinger, E. (1926). An undulatory theory of the mechanics of atoms and molecules. *Physikalische Zeitschrift*, **27**, 518–527.

[2] Bloch, F. (1929). Über die Quantenmechanik der Elektronen in Kristallgittern. *Zeitschrift für Physik*, **52**(7–8), 555–600.

[3] Anderson, P. W. (1958). Absence of diffusion in certain random lattices. *Physical Review*, **109**(5), 1492.

[4] Joos, E., Zeh, H. D., Kiefer, C., Giulini, D. J. W., Kupsch, J., Stamatescu, I. O. (2003). *Decoherence and the Appearance of a Classical World in Quantum Theory*. Springer.

[5] Kittel, C. (2004). *Introduction to Solid State Physics* (8th ed.). Wiley.

[6] Laughlin, R. B. (2005). *A Different Universe: Reinventing Physics from the Bottom Down*. Basic Books.

[7] Bekenstein, J. D. (1973). Black holes and entropy. *Physical Review D*, **7**(8), 2333–2346.

[8] Ashcroft, N. W., Mermin, N. D. (1976). *Solid State Physics*. Harcourt College Publishers.

[9] Georgescu, I. M., Ashhab, S., Nori, F. (2014). Quantum simulation. *Reviews of Modern Physics*, **86**(1), 153–185.

[10] Rovelli, C. (2004). *Quantum Gravity*. Cambridge University Press.

[11] Sarnowski, M. J. *Quantum Mechanics from Vacancy Defects in a Holosphere Lattice*, Holosphere Theory Paper 1, 2025.

[12] ’t Hooft, G. (2016). *The Cellular Automaton Interpretation of Quantum Mechanics*. Springer.

[13] Rovelli, C. (2004). *Quantum Gravity*. Cambridge University Press.

[14] Feynman, R. P. (1948). Space–Time Approach to Non-Relativistic Quantum Mechanics. *Reviews of Modern Physics*, **20**(2), 367–387.

[15] Bloch, I. (2005). Ultracold quantum gases in optical lattices. *Nature Physics*, **1**, 23–30.

[16] 't Hooft, G. (2014). The Cellular Automaton Interpretation of Quantum Mechanics. *arXiv preprint* arXiv:1405.1548.

[17] Rovelli, C. (2004). *Quantum Gravity*. Cambridge University Press.

[18] Lewenstein, M., Sanpera, A., Ahufinger, V., et al. (2007). Ultracold atomic gases in optical lattices: mimicking condensed matter physics and beyond. *Advances in Physics*, 56(2), 243–379.

[19] Weinberg, S. (1967). A model of leptons. *Phys. Rev. Lett.*, 19, 1264.

[20] Higgs, P. W. (1964). Broken symmetries and the masses of gauge bosons. *Phys. Rev. Lett.*, 13(16), 508–509.

Appendix A: Glossary of Terms

- **Angular Coherence**: The condition in which the rotational phase of neighboring Holospheres aligns sufficiently to allow coherent energy propagation and defect transfer.
- **Coherence Compatibility Index** (χ_c): A dimensionless parameter defined as $\chi_c = R_\phi / R$, indicating the relative coherence reach of a particle within the full Holosphere lattice.
- **Coherence Depth**: The number of nested lattice layers over which phase alignment is maintained for a given particle or wave mode. Determines tunneling reach and decoherence onset.
- **Coherence Gradient**: A spatial change in angular phase alignment across the lattice, which can result in directional tension, energy transfer, or gravitational-like strain.
- **Coherence Horizon**: The maximum radial distance over which a particle's phase remains in alignment with the surrounding Holosphere lattice, allowing coherent energy exchange and propagation.
- **Cuboctahedral Packing**: A dense geometric arrangement where twelve spheres surround one central sphere in a symmetrical structure; forms the local topology of the Holosphere lattice.
- **Dark Bosons**: Coherent orbital excitations formed from angular strain modes that are phase-incompatible with the observer's lattice layer, rendering them undetectable via electromagnetic coupling.
- **Defect Propagation**: The movement of a vacancy or strain discontinuity through the Holosphere lattice, enabling the emergence of quantum behavior such as wave interference and tunneling.

- **Holosphere**: A discrete, neutron-scale spinning spherical unit composed of Planck-scale lattice shells. Forms the building block of space, particles, and fields in the Holosphere Theory.
- **Inclusion Defect**: A topological distortion representing antimatter or unstable energy concentration, often phase-inverted or angularly mismatched compared to vacancy-type defects.
- **Lattice Strain**: Accumulated angular misalignment between Holospheres that generates tension, phase slippage, or effective field behavior (e.g., gravity, charge).
- **Orbital Mode**: A coherent motion of Holospheres or defects forming stable patterns (e.g., ring or triplet structures). Responsible for defining mass, charge, or spin properties.
- **Phase-Locking Radius** (R_ϕ): The radial distance within which a particle can maintain coherent angular phase alignment with the medium. Beyond this radius, phase mismatch disrupts coherence and transmission.
- **Quantum Triplet**: A structure composed of three coherently orbiting dark bosons around vacancy defects. Serves as the fundamental unit for fermions such as the electron.
- **Rotational Misalignment**: A deviation in angular phase between adjacent Holospheres. Large misalignments lead to decoherence or the emergence of massive gauge bosons.
- **Spin Tension**: A form of angular strain resulting from competing rotational directions in the lattice, underlying the emergence of mass and force-carrying interactions.
- **Vacancy Defect**: A missing Holosphere at a lattice site, generating angular phase distortion that behaves as a quantum particle (e.g., electron, neutrino) depending on orbital configuration.

ω: Angular frequency of a photon or coherent defect, measured in radians per unit time. Preferred over ω in Holosphere Theory due to its direct relation to rotational phase.

$v_{\mathbf{emit}}$: Angular velocity of the Holosphere lattice shell at the emission point; defines the local coherence speed of the medium.

c: Speed of light; corresponds to the boundary-layer coherence velocity in the Holosphere lattice.

b: Fractional lookback time, defined as $b = t/T$, where t is the lookback duration and T is the total lattice age.

$\exp(-b^3/3)$: Phase-drag factor due to accumulated coherence strain between lattice shells.

Glossary of Equations

Equation	Meaning / Description
$m^* = \frac{\hbar^2}{2Ja^2}$	Effective mass derived from the discrete hopping parameters in the lattice.
$i\hbar\frac{\partial\psi}{\partial t} = -\frac{\hbar^2}{2m^*}\frac{\partial^2\psi}{\partial x^2} + V(x,t)\psi$	Continuum limit Schrödinger-like equation emerging from the tight-binding model.
$\psi_{n+1} - 2\psi_n + \psi_{n-1} \approx a^2\frac{\partial^2\psi}{\partial x^2}$	Discrete second difference approximating the second spatial derivative in the wave equation.
$v(r) = \sqrt{C_0 r e^{-r/r_s} + C_c r e^{-r/r_d}}$	Hybrid velocity-redshift model from Holosphere Theory describing galactic rotation curves.

Appendix B: Comparative Framework for Quantum Interpretation

The following tables compare key features of standard quantum mechanics with their counterparts in the Holosphere Lattice framework, illustrating how discrete defect dynamics and angular coherence provide physically grounded alternatives to traditional interpretations.

Comparison: Standard Quantum Mechanics vs. Holosphere Lattice Model

1. Ontological Basis

The ontological assumptions of standard quantum mechanics treat the wavefunction as a fundamental, irreducible entity—existing in a high-dimensional configuration space, with no requirement for a physically structured background. Interpretations vary, but the mathematics does not mandate a discrete or geometric substrate.

By contrast, the Holosphere Lattice Model postulates that space itself is composed of discrete, rotating units—Holospheres—arranged in a cuboctahedral geometry. Quantum phenomena arise not from abstract wavefunctions but from the motion and interference of topological defects within this structure. This framework restores a realist, physically grounded ontology in which particles, fields, and wave behavior emerge from tangible rotational coherence and angular strain in a discrete spacetime medium.

Feature	**Standard Quantum Mechanics**	**Holosphere Lattice Model**
Foundation	Wavefunction as a fundamental mathematical object	Discrete lattice of Holospheres with dynamic packing defects
Origin of Quantum Behavior	Postulated wave-particle duality and probabilistic interpretation	Emergent from non-local interactions and spin dynamics of defects
Interpretation	Copenhagen, Many-Worlds, etc.	Real, physical model based on defect propagation and angular momentum transfer

Table 1: Comparison of foundational features between standard quantum mechanics and the Holosphere lattice model.

2. Physical Interpretation of Tunneling and Band Structures

Phenomenon	**Standard QM Interpretation**	**Holosphere Model Interpretation**
Tunneling	Probability amplitude penetrates classically forbidden region	Vacancy defects propagate through transient bosonic ring instabilities
Band Gaps	Destructive interference in Bloch wavefunctions in periodic potentials	Gaps emerge from symmetry constraints and spin-resonance in the packing lattice
Quantized Energy Levels	Solutions to boundary conditions in continuous potentials	Standing wave modes of discrete defect-lattice configurations

3. Vacuum and Particle Structure

Feature	**Standard QM**	**Holosphere Theory**
Vacuum	Continuous background with quantum fluctuations	Structured cuboctahedral lattice of spinning spheres
Potentials	External, imposed fields (e.g., harmonic, square well)	Emergent from internal defect distribution and symmetry breaking
Particles	Pointlike, intrinsic properties (mass, spin, charge)	Composite structures from nested ring defects and bosonic orbitals

Summary: While the equations governing wave propagation (e.g., Schrödinger, tight-binding models) appear mathematically similar, their physical foundations diverge. The Holosphere model provides a geometric and dynamical interpretation where quantum behavior arises from the discrete, spinning, and defect-laden structure of space itself.

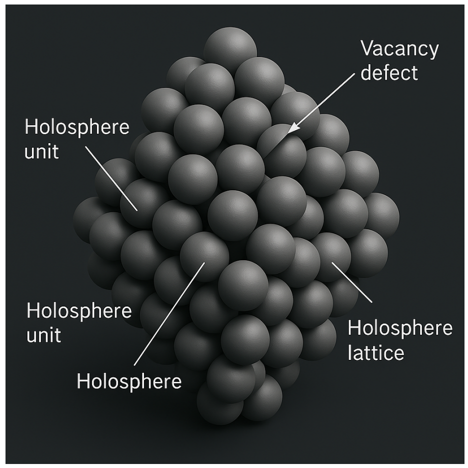

Figure 1: A 3D-rendered schematic illustrating nested spinning spheres forming a Holosphere lattice. The structure encodes both rotational symmetry and discrete vacancy defects, which are responsible for emergent quantum behavior. Defects propagate through the lattice, mimicking particle wavefunctions.

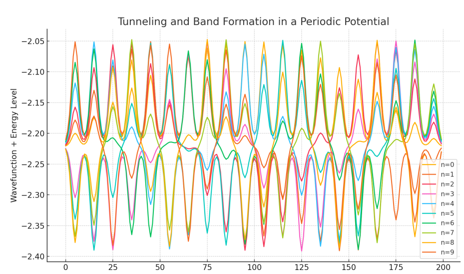

Figure 2: Here is a visualization showing how energy bands and tunneling behavior emerge from a periodic potential. Each curve corresponds to a low-lying eigenfunction shifted by its eigenenergy, demonstrating the localized and delocalized states forming under the influence of a lattice potential.

Appendix B: Derivation of Effective Mass from Angular Strain

In the Holosphere lattice model, mass is not treated as an intrinsic, irreducible property of matter, but as an emergent parameter derived from the angular strain experienced by propagating vacancy defects. This section outlines the derivation of the effective mass m^* from first principles based on lattice geometry, hopping energy, and angular phase continuity.

B.1 Lattice Hopping and Angular Coupling

Let a vacancy defect propagate across a cuboctahedral lattice composed of nested spinning Holospheres with lattice spacing a. The defect moves between nearest-neighbor sites via coherent angular coupling—i.e., it hops only when adjacent Holospheres are sufficiently aligned in spin and phase.

The hopping energy J is defined as the energy required for a defect to transfer angular momentum to a neighboring site. This energy arises from the torque needed to overcome angular misalignment and momentarily reconfigure the phase field.

We define the angular coupling between adjacent sites as:

$$J = \frac{\tau_{\text{eff}} \cdot \theta_{\text{min}}}{\Delta t},$$

where:

- τ_{eff} is the effective angular torque from the surrounding Holospheres,
- θ_{min} is the minimum phase angle required for coherent hopping,
- Δt is the angular response time of the lattice.

This relation reflects the physical cost of rotating the local coherence field to permit defect migration.

B.2 Tight-Binding Kinetic Term and Continuum Limit

In the tight-binding approximation, the evolution of a defect wavefunction $\psi_n(t)$ is governed by:

$$i\hbar \frac{d\psi_n}{dt} = -J\left(\psi_{n+1} + \psi_{n-1}\right) + V_n \psi_n.$$

Using the continuum approximation:

$$\psi_{n\pm1} \approx \psi(x) \pm a\frac{\partial \psi}{\partial x} + \frac{a^2}{2}\frac{\partial^2 \psi}{\partial x^2},$$

we substitute and simplify:

$$i\hbar\frac{\partial\psi}{\partial t} \approx -2J\psi + Ja^2\frac{\partial^2\psi}{\partial x^2} + V(x)\psi.$$

Dropping the constant term $-2J\psi$ into the effective potential, we compare this with the standard time-dependent Schrödinger equation:

$$i\hbar\frac{\partial\psi}{\partial t} = -\frac{\hbar^2}{2m^*}\frac{\partial^2\psi}{\partial x^2} + V(x)\psi,$$

yielding the effective mass:

$$m^* = \frac{\hbar^2}{2Ja^2}.$$

B.3 Angular Strain Interpretation

This effective mass is not fundamental, but a measure of the lattice's resistance to rotational reconfiguration. When a defect attempts to propagate, it must induce angular strain in surrounding Holospheres. The higher the local rotational coherence (i.e., the more rigid the phase alignment), the greater the hopping resistance, and the larger the effective mass.

Thus, the mass m^* serves as a proxy for the angular elasticity of the lattice. In Holosphere Theory, mass arises from the difficulty of transferring rotational phase—linking inertia directly to angular coherence strain.

B.4 Implications for Particle Families

Different generations of particles (e.g., electron, muon, tau) are modeled as the same topological charge structure (a triple-ring defect) surrounded by different orbital strain configurations. These differing strain environments modify J and a, and thus yield different effective masses:

$$m^*_{\text{generation}} \propto \frac{1}{J_{\text{gen}}a^2_{\text{gen}}}.$$

Therefore, particle mass differences across generations emerge from changes in angular strain geometry—without altering topological charge or introducing field-specific Yukawa couplings.

Appendix C: Holosphere Terms Compared to Quantum Field Theory

To assist readers trained in the language of quantum field theory (QFT), this appendix presents a side-by-side comparison of key terms, concepts, and structures from standard QFT and their corresponding interpretations in the Holosphere lattice model. This mapping helps clarify how the Holosphere framework reinterprets conventional notions of fields, particles, interactions, and spacetime.

Concept	**Quantum Field Theory (QFT)**	**Holosphere Theory**
Spacetime	Continuous Minkowski (or curved GR) manifold	Discrete cuboctahedral lattice of spinning Holospheres
Fields	Operator-valued functions over spacetime	Angular phase and coherence fields propagating across nested lattice layers
Particles	Excitations (quanta) of underlying fields	Coherent topological defects in rotational lattice geometry
Wavefunction ψ	Probability amplitude over position or momentum space	Defect amplitude across Holosphere lattice with coherence constraints
Gauge Bosons	Field quanta mediating forces (e.g., photons, gluons)	Orbital coherence pulses propagating angular strain across lattice layers
Higgs Field	Scalar field providing mass via symmetry breaking	Not required; mass emerges from orbital strain and phase misalignment
Vacuum Fluctuations	Zero-point energy and virtual particles in field modes	Rotational strain and stochastic hopping in the Holosphere coherence field
Renormalization	Absorbing infinities in perturbation theory	Avoided; lattice-based interactions are finite and geometric
Lagrangian Density	Fundamental quantity to derive field equations	Emergent angular action built from defect propagation and coherence gradients
Path Integrals	Sum over field configurations weighted by action	Defect paths through discrete angular phase space, bounded by coherence alignment
Local Interactions	Mediated by field operators at same spacetime point	Arise from coherent coupling between adjacent lattice sites via spin alignment
Symmetry Groups	Internal gauge symmetries (e.g., SU(3), SU(2), U(1))	Geometric angular symmetries of nested orbital arrangements and lattice projection
Antiparticles	Solutions with negative energy or charge conjugation	Time-inverted or angular-mismatched inclusion defects with unstable topology
Fermions	Half-integer spin fields obeying Pauli exclusion	Triplet ring defects forming coherent but phase-excluding orbital structures

Table 2: Conceptual mapping between Quantum Field Theory and Holosphere Theory.

C.1 Summary

While QFT treats particles as pointlike field quanta in continuous spacetime, Holosphere Theory reinterprets them as extended topological configurations in a discrete, rotating lattice. The key shift is from abstract operator fields to geometric strain, coherence, and spin alignment across a finite structure. This framework eliminates divergences, redefines mass and charge as geometric outcomes, and introduces a lattice-based mechanism for measurement, interaction, and unification.

Appendix D: Holosphere Mass Generation Compared to the Standard Model

The origin of particle mass is a central question in modern physics. In the Standard Model (SM), mass arises via interaction with the Higgs field, which provides mass through spontaneous symmetry breaking and Yukawa couplings. While this approach is mathematically successful, it leaves open questions about why the Yukawa couplings differ so dramatically between generations and why mass scales appear as they do.

In contrast, Holosphere Theory derives mass from the physical structure and angular strain of a discrete spacetime lattice. This appendix outlines the key differences between the two models and provides a coherence-based reinterpretation of mass generation.

C.1 Standard Model View: Mass from Higgs Coupling

In the SM, fermion masses are given by:

$$m_f = y_f \frac{v}{\sqrt{2}},$$

where:

- y_f is the Yukawa coupling for fermion f,
- $v \approx 246\,\mathrm{GeV}$ is the Higgs vacuum expectation value.

The Yukawa couplings y_f are treated as free parameters, tuned to match experimental data. This leads to large hierarchy gaps—for instance:

$$\frac{m_\mu}{m_e} \approx 206, \quad \frac{m_\tau}{m_\mu} \approx 17,$$

without deeper explanation from first principles.

D.2 Holosphere View: Mass from Angular Coherence Strain

In Holosphere Theory, mass arises from the difficulty of propagating topological defects through a discrete, spin-aligned lattice. Each charged particle is modeled as a stable configuration of three ring defects (triple-ring), surrounded by a nested orbital structure—called a dark boson orbital—that determines the effective angular stiffness of the surrounding medium.

The effective mass is given by:

$$m^* = \frac{\hbar^2}{2Ja^2},$$

where:

- J is the hopping energy determined by local angular strain and rotational resistance,
- a is the lattice spacing (e.g., Holosphere diameter, 1.3 fm),
- The mass increases with stronger coherence and decreased orbital flexibility.

Thus, the mass hierarchy among particle generations is explained as follows:

- The electron's triple-ring defect is surrounded by a relatively flexible orbital configuration (low J, high a),
- The muon's orbital is more tightly wound—greater angular strain, lower a, higher J,
- The tauon is even more tightly confined, resulting in the highest m^* among the three.

D.3 Comparison Table

Feature	**Standard Model (Higgs)**	**Holosphere Theory**
Mass Origin	Coupling to Higgs field via arbitrary Yukawa constants	Angular strain and phase stiffness of surrounding lattice
Free Parameters	13+ fermion Yukawa couplings	None; mass emerges from geometric and coherence structure
Generation Mass Gaps	Explained by fitting different couplings	Explained by different orbital strain layers in same defect topology
Charge Conservation	Requires symmetry constraints (gauge invariance)	Arises from topological conservation of ring defects
Mass–Charge Link	Independent parameters	Unified: same charge topology, different orbital strain
Experimental Predictions	No geometric insight into particle size or coherence	Predicts coherence length, mass ratio bounds, and strain distributions

D.4 Implications and Testability

Holosphere Theory predicts that:

- Particle mass depends on the coherence strain of orbital structures—not on coupling to a universal scalar field.
- All charged leptons (e.g., e^-, μ^-, τ^-) arise from the same triple-ring core but differ only in orbital strain configuration.
- A future fourth generation would require a coherence shell with much higher angular tension and may be unstable (see Paper 15).
- Mass variation should correlate with localized lattice strain, suggesting indirect measurables in coherence-based detectors.

In this view, mass is not added to a particle—it is encoded in the structure of the lattice medium surrounding the defect. The lattice resists acceleration of tightly bound orbitals more strongly, giving rise to higher inertial mass naturally.

Appendix E: Mass of Gauge Bosons in the Holosphere Lattice

In the Standard Model, the masses of the $W^\pm$ and Z^0 bosons arise from electroweak symmetry breaking via the Higgs mechanism. These bosons acquire mass through interactions with the Higgs field, while the photon remains massless due to unbroken $U(1)$ gauge symmetry.

Holosphere Theory offers an alternative, geometric explanation. In this model, the mass of a boson is not derived from symmetry breaking, but from the angular strain and coherence constraints required to propagate a particular excitation mode through the discrete Holosphere lattice.

E.1 Massless vs. Massive Bosons

In the Holosphere lattice:

- The **photon** corresponds to a phase-aligned triplet orbital that moves frictionlessly through the lattice, maintaining perfect angular coherence—resulting in zero effective mass.
- The **W and Z bosons** correspond to high-tension orbital modes that exhibit phase incompatibility or curvature strain with the surrounding lattice layers. This strain imposes an energetic cost for propagation, giving rise to a finite mass.

The boson mass therefore depends on:

- The **orbital misalignment energy** across lattice shells,

- The **number of coherence layers** the excitation traverses (coherence depth),
- The **angular curvature** required to maintain local symmetry within the rotational field.

E.2 Geometric Mass Formula

We define an effective boson mass from angular strain as:

$$m_B = \frac{\hbar^2}{2J_B a_B^2},$$

where:

- J_B is the angular hopping energy for the bosonic orbital mode,
- a_B is the effective coherence spacing (the boson's orbital wavelength or shell spacing).

For massless bosons (photons, gluons under ideal conditions), $J_B \to \infty$ or $a_B \to \infty$, causing $m_B \to 0$.

For W/Z bosons, which represent tightly strained orbital modes, J_B is finite and relatively small due to rotational resistance, and a_B is compact—resulting in a large mass:

$$m_W \sim 80\,\text{GeV}, \quad m_Z \sim 91\,\text{GeV}.$$

E.3 Boson Mass Ratios and Coherence Suppression

Holosphere Theory explains the difference in mass between the W and Z bosons as arising from differing degrees of angular symmetry:

- The Z^0 boson corresponds to a more symmetric orbital mode spanning multiple directions in the lattice, requiring greater total angular tension.
- The $W^\pm$ bosons correspond to chirally asymmetric configurations with less overall angular reach, yielding a slightly lower mass.

This geometric asymmetry explains the experimental ratio:

$$\frac{m_W}{m_Z} \approx \cos\theta_W \approx 0.88,$$

where θ_W is the Weinberg angle.

In Holosphere Theory, θ_W emerges as a geometric angle between coherence vectors in a spin-rotational lattice frame, not as a parameter from symmetry group mixing.

E.4 Comparison with Higgs-Based Mechanism

Feature	**Standard Model**	**Holosphere Theory**
Mass Generation	Spontaneous symmetry breaking via Higgs field	Angular coherence strain in rotating lattice
Gauge Fields	$SU(2)_L \times U(1)_Y$ mixed to $U(1)_{EM}$	Emergent from symmetry and phase-locking of orbital modes
Weinberg Angle	Empirical parameter from mixing matrix	Geometric angle from coherence vector projection
Massless Photon	Survives due to unbroken $U(1)$ symmetry	Survives due to perfect coherence and zero angular strain
Heavy W/Z Bosons	Gain mass via Higgs field interactions	Arise from rotational misalignment and coherence compression
Mass Ratio Prediction	Depends on fit parameters	Derived from geometric projection of phase-aligned vectors

Table 3: Comparison of gauge boson mass mechanisms in the Standard Model versus Holosphere Theory.

E.5 Physical Interpretation

Massive bosons in the Holosphere lattice are interpreted as short-range coherence pulses that cannot maintain alignment beyond a limited angular distance. Their propagation requires frequent reconfiguration of lattice spin structure, absorbing energy and reducing coherence lifetime. This naturally limits their range and explains why weak interactions are short-ranged compared to electromagnetic interactions.

E.6 Summary

The mass of gauge bosons in Holosphere Theory is not imposed by a field or symmetry breaking mechanism but emerges from the intrinsic coherence geometry of the discrete lattice. The photon is massless because it propagates without phase resistance. The W and Z bosons acquire mass because their configurations strain the surrounding Holospheres, inducing effective inertia and limiting coherence range.

This explanation is testable through correlations between boson mass, coherence length, and angular projection symmetry—and requires no scalar Higgs particle to generate mass from vacuum fields.

Appendix F: Fermion–Boson Coupling and Force Unification in the Holosphere Framework

In the Holosphere model, fundamental forces emerge from angular phase interactions between topological defects (fermions) and orbital excitations (bosons) within a rotating cuboctahedral lattice. This appendix outlines how boson-fermion coupling arises physically, how it leads to observable force behavior, and how it suggests a path toward geometric unification of interactions.

F.1 Coupling as Angular Phase Locking

Each charged fermion is modeled as a triple-ring topological defect orbiting a vacancy site, surrounded by a nested orbital of phase-coherent dark bosons. Bosons, in turn, are phase perturbations in the surrounding lattice structure—representing coherent angular field excitations.

Coupling between fermions and bosons occurs when:

- The phase angle of a propagating boson overlaps with a resonance mode of a triple-ring fermion orbital,
- Angular momentum exchange between bosonic coherence shells and fermionic defects becomes resonantly phase-locked,
- The orbital tension aligns in direction and timing with the lattice strain field of the fermion structure.

This results in a geometric version of "gauge interaction" via angular overlap and mutual coherence amplification.

F.2 Electromagnetic Interaction

The photon in Holosphere Theory is a triplet orbital with perfect phase coherence and no angular resistance. It couples to fermions by resonantly aligning with the outermost dark boson orbital, modulating the trajectory of ring defects via angular phase displacement.

Coulomb interaction arises as:

- Phase-aligned repulsion or attraction between overlapping ring defects mediated by orbital phase,
- A long-range torque field induced by photon triplets rotating synchronously with charge topology.

F.3 Weak Interaction

The W and Z bosons are tightly wound orbital pulses with high angular tension and limited coherence range. They couple to fermions only when:

- The internal dark boson orbital of a fermion enters a misaligned coherence state,
- Sufficient orbital compression occurs to momentarily support high-energy angular misalignment,
- The symmetry of the triple-ring is perturbed, allowing chirality-sensitive coupling.

This naturally explains the short range and flavor-changing properties of the weak force.

F.4 Geometric Force Unification

All known forces in Holosphere Theory are angular coherence phenomena, distinguished by:

- **Coherence depth:** The number of nested Holosphere layers involved in orbital excitation,
- **Strain threshold:** The angular resistance to phase alignment required to propagate the mode,
- **Topology of coupling:** Whether fermionic triple-rings are rotationally symmetric (EM), partially misaligned (weak), or contractively strained (strong).

Thus, force unification is not based on abstract group symmetries (e.g., $SU(3) \times SU(2) \times U(1)$), but on resonance conditions of rotating shells and angular phase geometry.

F.5 Summary Table

Interaction	**Standard Model Mechanism**	**Holosphere Interpretation**
Electromagnetism	$U(1)$ gauge symmetry, massless photon	Long-range triplet coherence with zero angular strain
Weak Force	$SU(2)$ symmetry, massive W/Z from Higgs field	Short-range high-strain boson coupling to defect misalignment
Strong Force	$SU(3)$ gluon exchange between color charges	Orbital confinement via packed angular strain and phase lock
Gravitation	Continuous spacetime curvature (GR)	Coherence gradient-induced strain field across large-scale lattice

F.6 Toward Full Unification

The Holosphere model opens the door to full force unification via:

- Angular coherence tensor fields (to replace gauge fields),
- Spinor-defect dynamics (fermions) embedded in phase-locked boson networks,
- Universal emergence of force via orbital resonance and coherence decay rate.

Rather than relying on symmetry groups, all forces become manifestations of angular strain propagation and resonance across discrete spinning units of space itself.

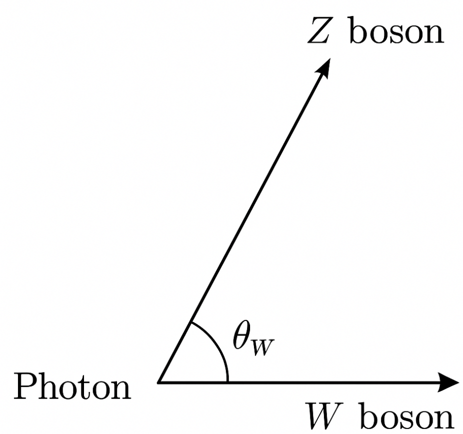

Figure 3: Geometric origin of the Weinberg angle θ_W in Holosphere Theory. The angle represents the projection of a neutral coherence excitation ($\vec{Z}$) onto phase-aligned and strained directions in the lattice. The electromagnetic mode ($\vec{E}$) is the perfect phase-aligned direction, while the W boson emerges from the orthogonal strain-resonant projection.